Structure and Stability of Molybdenum Sulfide Fullerenes†

M. Bar-Sadan,‡ A. N. Enyashin,§ S. Gemming,§,# R. Popovitz-Biro,|| S. Y. Hong,‡,▽ Yehiam Prior,⊥ R. Tenne,*,‡ and G. Seifert*,§

Departments of Materials and Interfaces and Chemical Physics and Electron Microscopy Unit, Weizmann Institute of Science, Rehovot 76100, Israel, and Physical Chemistry, Technische Universität Dresden, 01062 Dresden, Germany

Received: July 14, 2006; In Final Form: September 11, 2006

MoS_2 nanooctahedra are believed to be the smallest stable closed-cage structures of MoS_2, i.e., the genuine inorganic fullerenes. Here a combination of experiments and density functional tight binding calculations with molecular dynamics annealing are used to elucidate the structures and electronic properties of octahedral MoS_2 fullerenes. Through the use of these calculations MoS_2 octahedra were found to be stable beyond $n_{Mo} > 100$ but with the loss of 12 sulfur atoms in the six corners. In contrast to bulk and nanotubular MoS_2, which are semiconductors, the Fermi level of the nanooctahedra is situated within the band, thus making them metallic-like. A model is used for extending the calculations to much larger sizes. These model calculations show that, in agreement with experiment, the multiwall nanooctahedra are stable over a limited size range of 10^4-10^5 atoms, whereupon they are converted into multiwall MoS_2 nanoparticles with a quasi-spherical shape. On the experimental side, targets of MoS_2 and $MoSe_2$ were laser-ablated and analyzed mostly through transmission electron microscopy. This analysis shows that, in qualitative agreement with the theoretical analysis, multilayer nanooctahedra of MoS_2 with 1000−25 000 atoms (Mo + S) are stable. Furthermore, this and previous work show that beyond $\sim 10^5$ atoms fullerene-like structures with quasi-spherical forms and 30−100 layers become stable. Laser-ablated WS_2 samples yielded much less faceted and sometimes spherically symmetric nanocages.

1. Introduction

The synthesis of closed-cage carbon nanostructures—fullerenes and nanotubes—provoked the question regarding the stability of the corresponding inorganic fullerene nanostructures. Tungsten and molybdenum disulfide have layered structures similar to that of graphite. Hollow fullerene-like nanoparticles (IF) and nanotubes could be synthesized from these compounds and their respective metal diselenides.[1−3] Much experimental data concerning the synthesis and the characterization of WS_2 and MoS_2 nanotubes are currently available.[4,5] Theoretical investigations provided a basic understanding of their stability and their electronic and mechanical properties.[6−8] Numerous applications have been proposed for these nanomaterials, especially as superior solid lubricants and for impact-resistant nanocomposites, some of which have already been realized.[9]

Various strategies were proposed for the production of IF-MS_2 (M = Mo, W). The growth mechanisms of the nanoparticles were studied. These include the gas-phase reaction between H_2S and MoO_{3-x},[10] the solid-state reaction between MoO_3 nanobelts and sulfur at high temperatures,[11] sonoelectrochemical synthesis,[12] micelle-assisted synthesis,[13] and fabrication via an arc discharge in solutions.[14] It is necessary to note that most of these nanoparticles have an onionlike structure and possess an irregular faceted shape. The experimental investigations of the fullerene-like modification of MoS_2 went much further than the synthesis alone and also included quite detailed physical characterization. In particular, the fullerene-like MoS_2 nanoparticles were characterized by methods such as powder X-ray diffraction (XRD),[15] scanning tunneling microscopy (STM), high-resolution transmission microscopy (HRTEM),[16,17] visible spectroscopy,[18] and Raman and IR spectroscopy.[19] Intercalation and de-intercalation of alkali metal atoms into the MoS_2 fullerene-like lattice were also studied.[20] From the application viewpoint, the superior tribological properties of hollow MoS_2 and WS_2 nanoparticles offer a very large number of applications of these materials.[21] Furthermore, the high impact resistance of these nanoparticles offers numerous other applications.[22] Therefore, theoretical modeling, which may lead to a better understanding of the stability and the electronic properties of the IF nanomaterials, is highly warranted at this point. A number of first principles studies of MS_2 nanotubes have been undertaken,[6−8] but a systematic first principles study of the fullerene-like structure is not available so far.

Bulk synthesis of the IF normally yields nanoparticles with quasi-spherical shapes made of 30 molecular layers or more and an outer diameter of 30 nm or greater. Early work indicated that small hollow clusters of MoS_2 come often in octahedra and tetrahedra structures.[2,23] Indeed, laser ablation was used to produce some MoS_2 nanoparticles with an octahedral shape, ca. 2−5 nm in size, which were thought of as the "true inorganic fullerenes"[24] (see also Figure 1); i.e., these closed-cage nanoparticles are thought of as the genuine analogue of C_{60} in inorganic layered compounds. A detailed understanding of their structure at an atomistic level and their physicochemical behavior is still lacking, which is the focus of the present combined theoretical and experimental work.

† Part of the special issue "Arthur J. Nozik Festschrift".

* Authors to whom correspondence should be addressed. E-mail: reshef.tenne@weizmann.ac.il; Gotthard.Seifert@chemie.tu-dresden.de.

‡ Department of Materials and Interfaces, Weizmann Institute of Science.

§ Physical Chemistry, Technische Universität Dresden.

|| Electron Microscopy Unit, Weizmann Institute of Science.

⊥ Department of Chemical Physics, Weizmann Institute of Science.

Present address: FZ Rossendorf, P.O. Box 510119, 01314 Dresden, Germany.

▽ Present address: Department of Chemistry, University of Oxford, South Parks Road, Oxford OX1 3QR, U. K.

10.1021/jp0644560 CCC: $33.50
Published on Web 10/31/2006

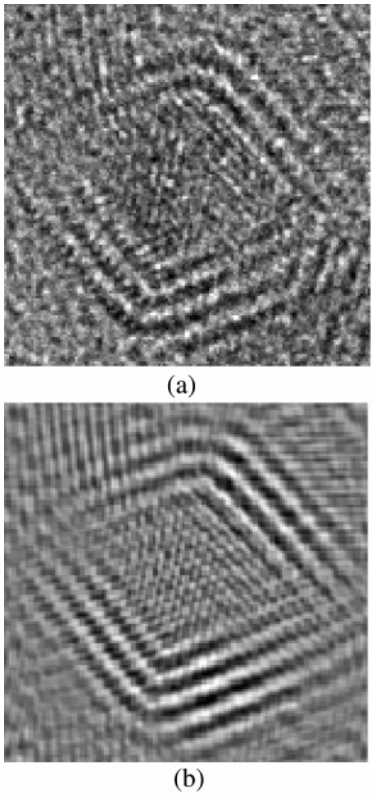

Figure 1. (a) Typical HRTEM micrograph of an octahedral MoS_2 nanoparticle and (b) its fast Fourier transform filtered image.

Despite the large amount of experimental data, theoretical studies of the MoS_2 fullerene-like structures are rare. A continuum model has been suggested, showing that dislocations and grain boundaries are intrinsic features of nested fullerene-like structures.[25] The presence of defects, such as double-coordinated sulfur atoms and MoS_6 prisms connected by the plane but not the edges (square-like defect), can explain in principle the variety of the fullerenic shapes observed in the experimental data.[26] The number of the structural models describing the octahedral structures can be expanded further by the possible presence of octahedral coordination in the MoS_6 units in the fullerene-like cages.[27] It is obvious though that unless a first principles methodology is being employed any attempt to make a comparison with the experimentally observed nanostructures and calculate their physical characteristics is of a limited scope.

The aim of the present work is to present the first detailed quantum mechanical calculations of MoS_2 nanoparticles with octahedral structures and compare the results of the computations with the available experimental data. The stability and electronic structure of the octahedral nanostructures with different stoichiometries and different construction principles for their walls and corners are studied. Additionally, these calculations are used for a model describing the stability of the stoichiometric octahedral MoS_2 fullerenes and the corresponding nanoplatelets. They permit a direct comparison with experiment, where structural changes from octahedral (faceted) nanoparticles 3−5 layers thick into quasi-spherical structures with 30 layers and greater are observed when their diameter grows beyond several nanometers. These remarkable changes are not limited to structure only. Ample theoretical evidence is presented, and hints in the experimental work show that while the platelets and the large (>30 nm) fullerene-like nanoparticles are semiconducting the nanooctahedra are in fact metallic-like. In this work a distinction is made between symmetric closed structures, which are named fullerenes, and closed but irregular structures, which are designated as fullerene-like structures.

2. Methods

Synthesis. Powders of MoS_2 (Sigma Aldrich, 99.5% pure), $MoSe_2$ (Alfa Aesar, 99.9% pure), and WS_2 (Alfa Aesar, 99.8% pure) were pressed into a target pellet (diameter 17 mm). The target was placed inside a quartz tube reactor heated to 450−700 °C. Pulsed laser ablation was conducted using a mildly focused, frequency-doubled Nd:YAG laser (532 nm, 10 Hz, 8 ns, ∼60 mJ per pulse) for 20 min. The focused spot was scanned continually across the pellet surface. The generated soot was flushed back downstream by flowing argon/helium gas and was collected on a quartz substrate, which was placed on a finger outside the oven. The gas flow rate was set to 200 cm^3 min^{-1} at atmospheric pressure. Numerous attempts to purify the nanooctahedra from the rest of the nanoparticles were carried out, however unsuccessfully so far.

The collected powder was sonicated in ethanol, placed on a carbon/collodion-coated Cu grid, and analyzed by TEM (Philips CM-120, 120 kV). Extensive work with TEM in the past shows that fullerene-like MoS_2 nanoparticles and nanotubes are very stable against beam damage under normal working conditions. As for the nanooctahedra the beam damage was studied as well in the present work. It was found that the nanooctahedra are stable against damage from the electron beam. Furthermore, HRTEM (FEI Tecnai F-30, 300 kV) was used together with Gatan imaging filtering (GIF) for electron energy loss spectroscopy (EELS). Beam damage (sulfur loss) occurred only after long exposure of an individual nanooctahedron under high-resolution imaging conditions. Some amorphous MoS_x between the octahedra, which is collected on the substrate during the laser ablation experiments and is transferred to the TEM grid, is inevitable. Therefore, during the HRTEM/EELS experiments the beam was focused to a frame with few nanooctahedra in proximity so as to minimize the influence of the amorphous material on the analysis. Energy-dispersive X-ray spectroscopy (EDS, EDAX Phoenix) was used as well.

Models and Computational Methods. The stoichiometric MoS_2 fullerene structures can be constructed by introducing defects to a monolayer of the trigonal prismatic MoS_2. Such defects are represented by the change of the regular motif of the MoS_6 trigonal prisms composing a monolayer without a change of the stoichiometry. Namely, the change of the coupling of the MoS_6 units from "triplets"—as in the layered MoS_2—into "pairs", "quadruplets", and "quintuplets" leads to square-, octagonal-, and decagonal-like defects, respectively. It follows that only square-like defects can form a surface with positive curvature making up the corners of closed-cage polyhedra.

Among the regular and semiregular polygonal solids one can distinguish between four morphological objects, whose edges terminate in corners made up of four faces. They are composed of triangular, square, and pentagonal faces (Figure 2). The fullerene MoS_2 structures with such shapes should have a square-like defect at each corner and octagonal (Figure 2.2) or decagonal (Figure 2.3) defects in the middle of the square or pentagonal faces, respectively. However, the triangular faces are fragments of the regular MoS_2 monolayer without any defect.

As shown in Figure 3, there are two ways for "cutting" triangular faces, which explains the existence of two families in each morphological type shown in Figure 2. In the first case (I) the Mo−S bonds are perpendicular to the edges. In the second case (II) the Mo−S bonds are parallel to the edges. The size, namely, the length of an edge of the fullerene structure, is

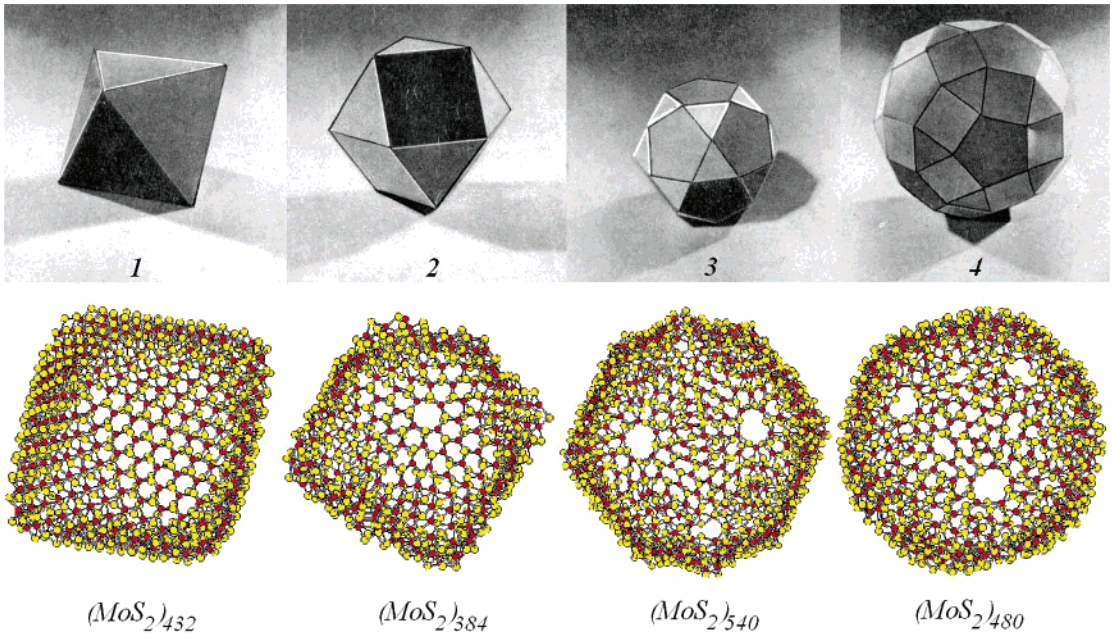

Figure 2. Possible structures of the MoS_2 fullerenes with regular (1, octahedron) or semiregular shapes (2, cuboctahedron; 3, icosadodecahedron; 4, rhomboicosadodecahedron). Red represents Mo, and yellow represents S.

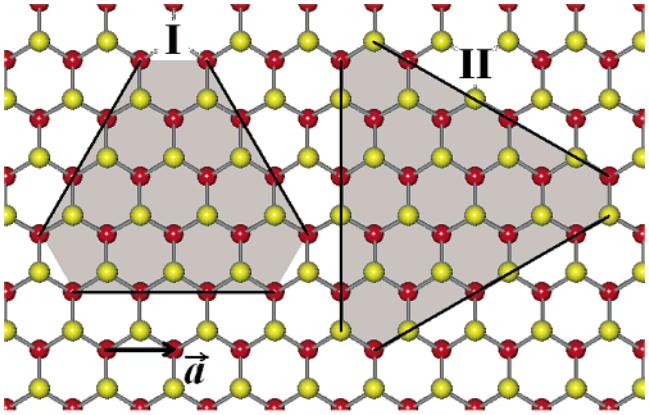

Figure 3. Structure of a hexagonal MoS_2 monolayer with the lattice constant $\bar{a}$. The variants (I and II) for the construction of the fullerenic facets are indicated by gray shaded areas. In case I the edges are along the (1−100) face while in case II they are along the (1−210) face.

determined by the number of hexagons that intersect the edge, "cutting" (Figure 3). Analysis of the HRTEM data of many nanooctahedra confirmed that only case I is relevant to the present study (vide infra). Therefore, no further information on case II is included in the present paper. The starting point for much of the present work is fullerene nanoparticles that are stoichiometric and possess octahedral shapes.

The stability and electronic structure of nonstoichiometric molybdenum sulfide fullerene nanoparticles with both a deficiency and a surplus of the sulfur content are also considered. The first detailed models for these fullerene nanoparticles were offered in ref 27. They are constructed with defects allowing closure in accordance with Euler's theorem, i.e., made of six rhombi at their corners. They have Mo and S atoms with coordination numbers that differ from those existing in the lattice of the bulk material. Besides these nanoparticles,[27] we consider here nanoparticles having the same motif for the walls and edges but another construction of their corners that seems to be less reactive. Particles with both prismatic and octahedral or mixed coordination of the Mo atoms are included. Through the use of the same designations offered by Parilla et al.,[27] the structures of all fullerene nanoparticles with an octahedral shape, which are investigated in the present study, are shown in Figure 4.

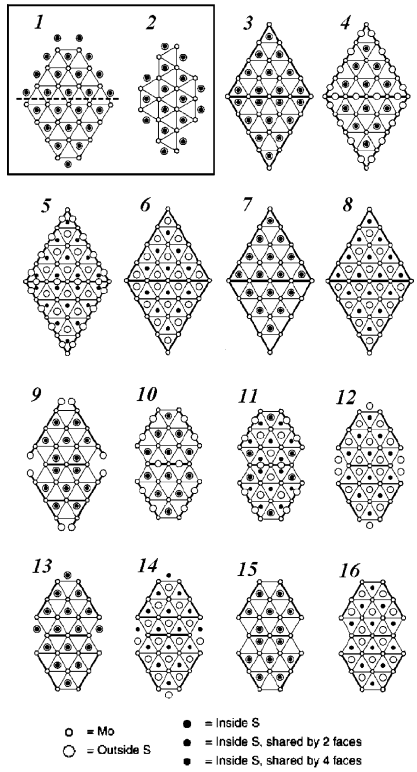

Figure 4. Schematic presentation of the cages of the stoichiometric (1 and 2) and nonstoichiometric (3−16) fullerenes of molybdenum sulfide considered in this work. Models 3−8 are offered by Parilla et al.[27]

All of the stability and electronic structure calculations were performed with the density-functional-based tight-binding (DFTB) method.[30,31] Before the full geometry optimization with the DFTB method the structures were preoptimized with a proprietary molecular mechanics (MM) force field. Finally, the stability of the optimized structures was verified by molecular

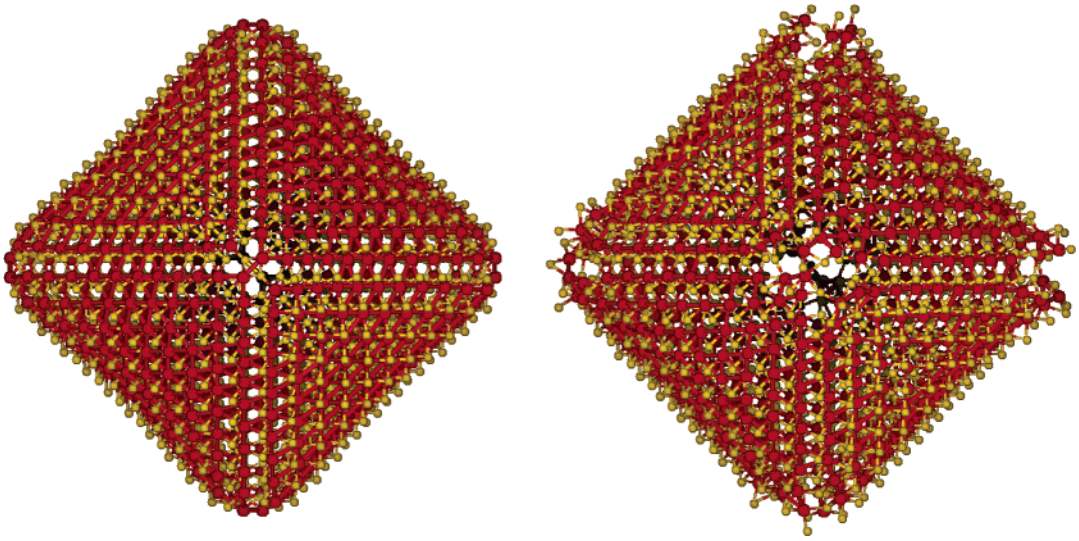

Figure 5. Optimized structure of the $(MoS_2)_{576}$ fullerene degraded to $Mo_{576}S_{1140}$ (on the left) and the skeleton $Mo_{576}S_{1140}$ after a MD simulation at 300 K (on the right) (DFTB calculations). Red represents Mo, and yellow represents S.

dynamics (MD) simulations. All energies are given in hartree units (H); 1 hartree = 27.2114 eV.

3. Results and Discussion

First, the stoichiometric fullerenes $(MoS_2)_x$ with octahedral structures and x = 12, 16, 36, 48, 64, 100, 108, 144, and 576 were considered. After geometry optimization it was realized that the small octahedral fullerenes (with $x \leq 64$) are unstable. Particularly, holes are formed in the walls of the octahedral polyhedron; i.e., a fraction of the sulfur atoms become 2-fold coordinated in the corners. However, on the whole the hollow octahedron structure of these fullerenes is preserved. After a MD simulation over 2 ps at T = 300 K these particles become unstable and loose their integrity.

The hollow structures of the higher $(MoS_2)_x$ nanooctahedra with $x \geq 100$ (and with diameters >2.0 nm) are found to be stable, but the Mo/S composition degrades to Mo_xS_{2x-12} due to "evaporation" of two S atoms from each of the six corners. The MD simulations at 300 K show a considerable distortion of the initial structure around the corners, but the fullerene-like facets and edges preserve their integrity (Figure 5). This result can be attributed to the high strain energy in the corners of a nanooctahedron. It further explains the absence of small (<2.0 nm) MoS_2 nanooctahedra in the laser-ablated soot (vide infra). The elastic energy in the nanooctahedra is appreciably larger than the strain in MoS_2 nanotubes that are 1−2 nm in diameter.[7] The presence of substoichiometric (with respect to S) corners makes the nanooctahedra with more than 100 Mo atoms (>2.0 nm) energetically more favorable. The presence of defects at the corners also should have a strong influence on the electronic properties of these systems (vide infra).

Another possibility to construct stable fullerene structures with a symmetric shape consists of changing the ratio between the number of S atoms outside and inside the Mo octahedral framework. Obviously, such a construction principle will also lead to large deviations from the 1:2 (Mo/S) stoichiometry. The first discussion of geometric models of such nonstoichiometric metal chalcogenide nanooctahedra can be found in ref 27. In the construction principle of such structures Mo−S coordinations are considered, which differs from that of bulk 2H−MoS_2 (Figures 4.3−4.8). These structures are found to be energetically unfavorable and are expected to lead to nanoparticles with high chemical reactivities. A more plausible construction principle considers particles with stoichiometric 1:2 (Mo/S) facets but with edges and corners deviating from such stoichiometries. This is realized by inner sulfur atoms at the edges shared between two facets and the one in the corner shared between four facets (Figures 4.9−4.16). Mo_nS_m nanooctahedra with n = 12, 18, 32, 38, 60, 66, 96, 102, 140, and 146 and $m/n \approx 0.78-2.67$ were investigated.

The nonstoichiometric fullerene-like particles differ in their S/Mo ratios even in the same series (Figure 4.2−4.16). Therefore, a simple comparison of the binding energies of nanooctahedra with the same number of Mo atoms is not a useful energetic criterion for the relative stability. An alternative possibility is to consider the energy of formation of these particles

$$\Delta E = \frac{E_t(Mo_nS_m) - n\epsilon_i - \left(\frac{m-2n}{8}\right)E_t(S_8)}{n+m} \qquad (1)$$

where $E_t(Mo_nS_m)$ and $E_t(S_8)$ are the energies of the fullerene Mo_nS_m and the sulfur octamer S_8 and ϵ_i is the energy (per atom) of an infinite MoS_2 monolayer.

The dependence of ΔE on the particle size for the various series of fullerene structures is shown in Figure 6. As the size of the fullerenes increases their stoichiometry tends to Mo/S = 1:2, because the number of atoms on the facets grows faster than those on the edges and corners. In addition, as in the case of carbon fullerenes one might expect a linear correlation between ΔE and $1/N$ (where $N = n + m$ is the total number of atoms in a fullerene cage) with ΔE approaching zero for $N \rightarrow \infty$.[32] But there is no such clear correlation between these quantities for all kinds of the Mo_nS_m particles. In general, the energy of formation of the nanoclusters is decreasing with $N \rightarrow \infty$. One also notices a large variation of ΔE for small clusters ($n < 38$).

The dependence of ΔE as a function of the stoichiometry of the Mo_nS_m octahedral fullerenes is shown in Figure 7. In a given series of structures a linear correlation between ΔE and the deviation from stoichiometry is clearly observed to be approaching zero at nominal stoichiometry. Considering the fact that the deviation from stoichiometry is limited to the corners and edges of the nanooctahedra, it is clear that with increasing size the strain energy of the cages is decreasing and the composition of the nanoclusters is approaching the 1:2 stoichiometry.

According to Figure 6 the most stable series of fullerenes are those of types 3, 4, 5, 9, 12, and 15 (Figure 4), which

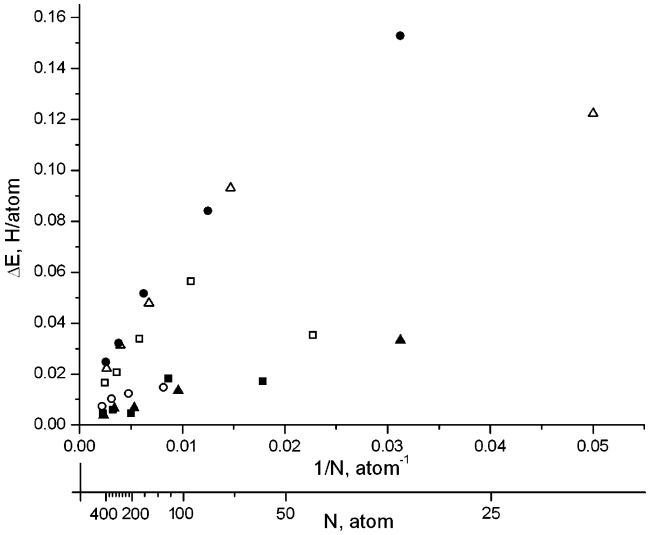

Figure 6. DFTB-calculated energies of formation of the MD stable Mo_nS_m fullerenes (ΔE) as a function of $1/N$ ($N = n + m$ from 20 up to 600 atoms) (●, type 3; ○, type 4; ■, type 5; □, type 9; ▲, type 12; △, type 15 as shown in Figure 4).

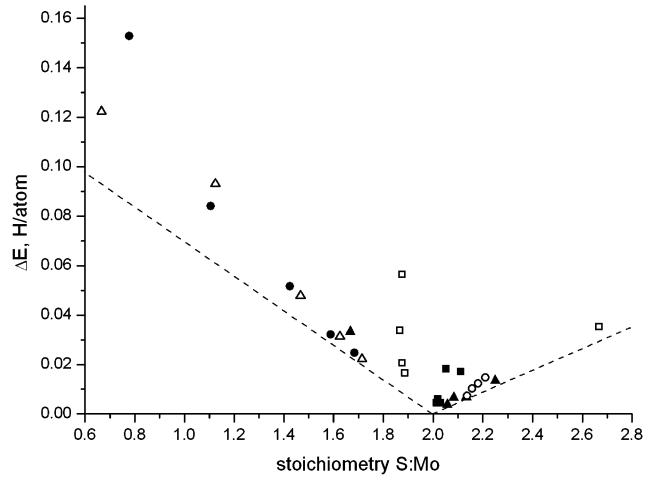

Figure 7. DFTB-calculated energies of formation of the MD stable Mo_nS_m fullerenes (ΔE) as a function of the stoichiometry (S/Mo = m/n) in the range for $N = n + m$ up to $N = 600$ (●, type 3; ○, type 4; ■, type 5; □, type 9; ▲, type 12; △, type 15 as shown in Figure 4). The Mo_nS_m fullerenes are unstable underneath the dashed lines.

confirms the qualitative considerations of Parilla et al.[27] Some of the structures have a stoichiometry down to Mo/S = 1:1.6, quite far from the stoichiometry of 2H−MoS_2. These rather stable structures can be divided into two groups: (1) cages with trigonal prismatic coordination of the Mo atoms (types 3, 9, and 15) and S atoms shared with two fullerenic faces and (2) cages with octahedral coordination of the Mo atoms (types 5 and 12). Interestingly, nanooctahedra with octahedral coordination in the MoS_6 units (types 5 and 12) are more stable than those with a trigonal prismatic coordination of the molybdenum, which occurs in the bulk 2H−MoS_2 phase. Octahedral coordination exists also in the bulk 1T−MoS_2 polytype, which has been obtained by intercalation/exfoliation of MoS_2 platelets. The authors of ref 27 have suggested that the stability of fullerenic 1T−MoS_2 polytypes could be higher than that of 2H−MoS_2, because octahedral coordination (1T) within octahedral particles of the Mo atoms in this case is sterically preferable. This conjecture is supported by the present calculations. The optimized hollow octahedral structures 3, 5, 9, 12, and 15 (Figure 4) are shown in Figure 8. MD simulations of these fullerene MoS_2 nanoparticles at 300 K confirmed their stability, where only slight distortions occur after the MD simulations at $T =$ 300 K. Thus, the present calculations do not exclude a possibility that the smallest nanooctahedra of molybdenum sulfide with octahedral coordination of the Mo atoms are stable and could coexist with particles based on the 2H−MoS_2 modification.

Recently, very small charged Mo_nS_m clusters of a composition close to MoS_2 were investigated by DFT calculations.[33] $Mo_{13}S_{25}^-$ and $Mo_{13}S_{28}^-$ clusters with a cage-like structure were found to be stable. Small Mo_nS_m clusters with $n = 12$, made of a Mo core and covered by S atoms but with an octahedral symmetry of the cage, were also studied. Geometrical optimization and MD simulations showed that $Mo_{12}S_{32}$ and $Mo_{12}S_{20}$ clusters of this type are also stable. However, these nanoclusters cannot be considered as "true inorganic fullerenes", because their structure does not resemble MoS_2 monolayers of the 2H− or 1T− MoS_2 polytypes.

The electronic density of states (DOS) of the nonstoichiometric fullerenes of molybdenum sulfide structures are shown in Figure 9. The DOS profiles of the fullerene-like structures are quite similar to those of semiconducting MoS_2 nanotubes and the corresponding bulk layered (2H) structure.[7] Despite this great similarity, however, it can be seen that all the hollow nanoparticles considered here exhibit metal-like character. The gap between the highest occupied and lowest unoccupied molecular orbitals (HOMO−LUMO gap) is very small and does not exceed a few 0.01 eV, independent of the nanocluster size and their stoichiometry. Generally, the valence band and the states around the HOMO of the Mo_nS_m fullerenes consist predominantly of 4d Mo states. For the fullerenes having only square-like defects at the corners (types 1 and 2 in Figure 4) these states are mainly localized at the atoms of these defects. Thus, in contrast to the MoS_2 (WS_2) nanotubes and the larger ($d \geq 30$ nm) quasi-spherical multilayer fullerene-like nanoparticles, which are semiconducting,[6,16,18] the present work shows that the MoS_2 nanooctahedra exhibit metallic-like character.

Mulliken charge distribution analysis shows that the charges in the octahedral fullerenes are close to those of a MoS_2 monolayer or a nanotube, where they are $-0.453e$ and $+0.906e$ for the S and Mo atoms, respectively.[6] For a fullerene (for example, $Mo_{576}S_{1140}$ of type 1, Figure 4) one obtains a charge transfer from Mo to S on average of $-0.41e$ and $-0.47e$ for the internal and external S atoms, respectively, and $+0.91e$ for the Mo atoms. The small difference between the charges of the external and the internal S atoms is the same as that for the MoS_2 nanotubes.[6]

A direct systematic investigation of the stability of molybdenum sulfide fullerene-like particles with quantum mechanical calculations in the size region of several thousands of atoms is impossible. Therefore, a phenomenological model for the energetics and the structural stability of MoS_2 nanoparticles with a fullerene-like structure was developed. This model bears some similarly to a corresponding model, which was successfully used to predict the stable structure of MoS_2 and WS_2 nanotubes and TiO_2 nanoscrolls.[7,34]

Fullerene structures with octahedral shapes can be characterized by six square-like defects (vide supra). The facets of these structures can be represented as monolayered nanoplatelets with triangular shapes. Indeed triangular MoS_2 nanosheets were experimentally observed.[35,36] The total energy of such octahedral structures E_f can be written as

$$E_f = N_i\epsilon_i + N_r\epsilon_r + N_p\epsilon_p \qquad (2)$$

where $N = n + m$ is the number of Mo and S atoms and N_i, N_r,

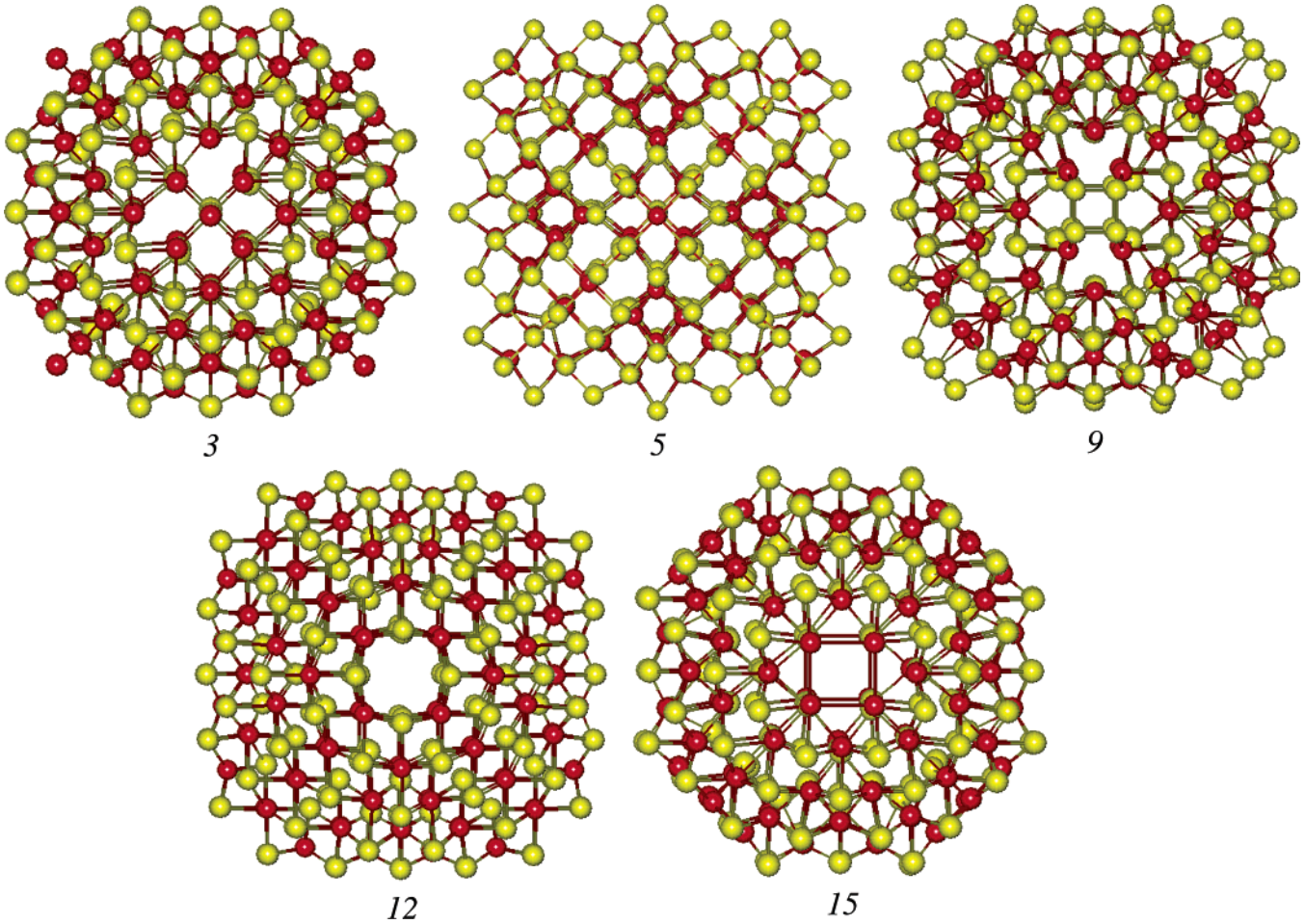

Figure 8. Structure of the stable types of nonstoichiometric fullerenes after MD simulations at 300 K (DFTB calculations): $Mo_{102}S_{162}$ (type 3, Figure 4), $Mo_{102}S_{206}$ (type 5), $Mo_{96}S_{180}$ (type 9), $Mo_{96}S_{200}$ (type 12), and $Mo_{96}S_{156}$ (type 15). Red represents Mo, and yellow represents S.

and N_p are the corresponding numbers of atoms at the facets, edges, and the corners, respectively. The sum $N_i + N_r + N_p$ gives the total number of atoms N. ϵ_i, ϵ_r, and ϵ_p are the corresponding energies per atom. The energy E_f for a fullerene structure, as shown in Figure 4.2 may then be expressed as

$$\frac{E_f}{N} = \frac{(\sqrt{N} - 6)}{\sqrt{N}}\epsilon_i + \frac{(6\sqrt{N} - 36)}{N}\epsilon_r + \frac{36}{N}\epsilon_p \qquad (3)$$

The energies can be calculated by using the DFTB method. ϵ_i is equal the energy/atom in a two-dimensional (2D) infinite MoS_2 hexagonal layer. According to the DFTB calculations this value is equal to -2.1542 H/atom.[7] For the determination of ϵ_r, the energy per atom of the edge atoms, the total energies E_t of infinite MoS_2 nanotubes with polygonal sections ("faceted" nanotubes) were calculated. These nanostructures modeled as infinite ones do not have any dangling bonds and give a good possibility to find ϵ_r as a function of the dihedral angle θ between two facetes of a polygonized nanotube or a fullerene. For a nanotube with a "faceted" structure, the energy E_t may be written as $E_t = N_i\epsilon_i + N_r\epsilon_r$, where N_i and N_r are the number of atoms at the facet and along the edge, respectively. For example, E_t for (24,0) MoS_2 nanotubes with polygonal cross-sections (triangle, square, hexagon, octagon, and dodecagon) were calculated (Figure 10). From these calculations the function $\epsilon_r = f(\theta)$, Figure 10, can be determined for each θ value. A quadratic fit gives for an angle $\theta = 109.47°$, the dihedral angle between the facets in an octahedral fullerene, $\epsilon_r = -2.1008$ H/atom.

To determine ϵ_p, the energies per atom of a 2D hypothetical square-octagonal layer of MoS_2 (ϵ_{p1}), a corresponding planar cluster Mo_4S_8 (ϵ_{p2}), and an Mo_4S_8 cluster, distorted as in the fullerenic apex (ϵ_{p3}), were calculated (the corresponding structures are shown in Figure 11). The energy ϵ_p can be expressed as: $\epsilon_p = \epsilon_{p1} + (\epsilon_{p2} - \epsilon_{p3})$. The calculations give $\epsilon_{p1} = -2.1464$ H/atom and $(\epsilon_{p2} - \epsilon_{p3}) = 0.1288$ H/atom. This gives $\epsilon_p = -2.0176$ H/atom.

For a description of the energetics of the multiwalled fullerene-like structures one has to take into account also the van der Waals interaction between the shells. This has been done with a model similar to that in ref 7. With ϵ_{vdW} as the interlayer van der Waals energy/atom, the total energy per atom for a multiwall octahedral fullerene with the number of shells equal to k may then be written as

$$\frac{E_f}{N} = \frac{\epsilon_i \sum_{j=1}^{k} \sqrt{N_j}(\sqrt{N_j} - 6) + \epsilon_r \sum_{j=1}^{k}(6\sqrt{N_j} - 36) + 36\epsilon_p k}{\sum_{j=1}^{k} N_j} + \frac{k-1}{k}\epsilon_{vdW} \qquad (4)$$

Here N_j is the number of atoms in the jth sheet. The value of ϵ_{vdW} is taken as twice the measured surface energy of MoS_2.[37] This gives $\epsilon_{vdW} = -0.0074$ H/atom, which is certainly only a rough estimate. The difference between N_j and N_{j-1} of these

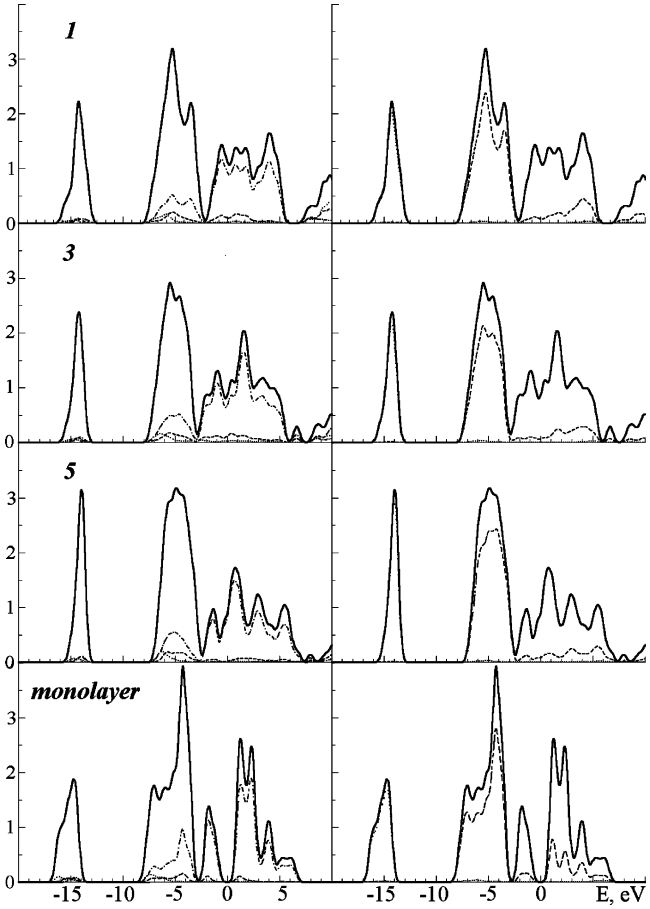

Figure 9. Densities of states of some nonstoichiometric fullerenes (DFTB calculations), $Mo_{100}S_{188}$ (type 1, Figure 4), $Mo_{102}S_{162}$ (type 3), and $Mo_{102}S_{206}$ (type 5) in comparison with a semiconducting MoS_2 monolayer (left panel, Mo states; right panel, S states, total DOS; dash−dotted line, d states, dashed line, p states, dotted line, s states).

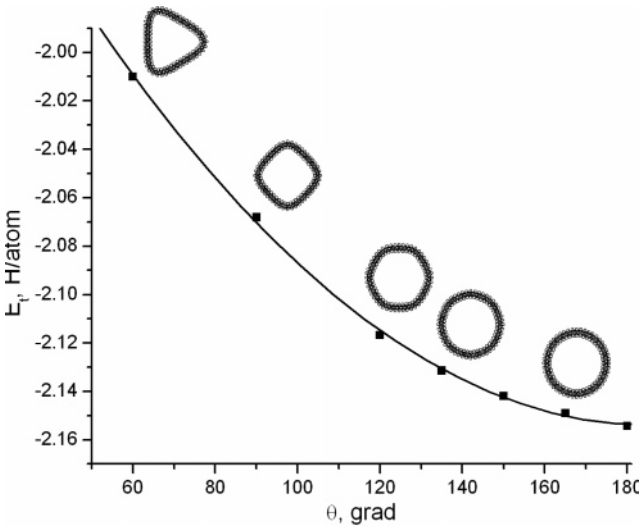

Figure 10. Energies of "faceted" MoS_2 nanotubes as a function of the dihedral angle θ between "facets". The data are obtained for a (24,0) MoS_2 nanotube, as an example, within the DFTB method and constrained geometry optimization.

octahedral fullerenes can be estimated using the lattice constants of bulk MoS_2

$$\sqrt{N_j} - \sqrt{N_{j-1}} = 3\sqrt{2}\,\frac{c}{a}$$

It is also important to estimate the relative stabilities of the

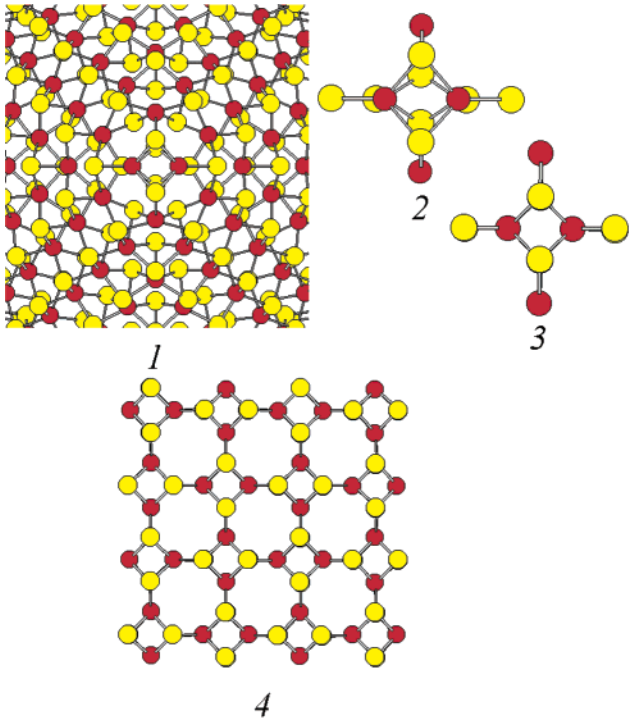

Figure 11. (1) Structure of the ideal stoichiometric MoS_2 fullerene-like apex with a square-like defect. (2) Model cluster (Mo_4S_8) of the square-like defect. (4) A hypothetical square-octagonal layer of MoS_2, constructed from the undistorted geometry (3) of the cluster (2). For 3 and 4 only the sulfur atoms above the Mo atomic layer are shown. Red represents Mo, and yellow represents S.

fullerene-like structures in comparison to those of monolayered triangular nanoplatelets, which are the building blocks of the facets of the octahedral fullerenes (Figure 3.II). Each of the Mo atoms at the edge of a nanoplatelet has two dangling bonds, adversely affecting its stability. On the contrary, in the fullerene-like shells locations of high strain (corners and edges) exist. The balance between the two kinds of chemically activated atoms determines the relative stability of the two kinds of nanostructures.

The total energy of a nanoplatelet, E_{np}, may be written as

$$E_{np} = N_i\epsilon_i + N_{xr}\epsilon_{xr} + N_{xp}\epsilon_{xp} \tag{5}$$

$$\frac{E_{np}}{N} = \frac{\sqrt{1+8/9N}-3}{\sqrt{1+8/9N}+1}\epsilon_i + \frac{36\sqrt{1+8/9N}-27}{8N}\epsilon_{xr} + \frac{9}{N}\epsilon_{xp} \tag{6}$$

where ϵ_{xr} and ϵ_{xp} are the energies per atom of atoms with unsaturated bonds at the edges and the apexes (corners) of such nanoplatelets. The total number of atoms is $N = N_i + N_{xr} + N_{xp}$, where N_i, N_{xr}, and N_{xp} are the numbers of inner (bulk) atoms, the atoms at the edges, and the atoms at the apexes, respectively. Equation 5 shows a linear dependence of the difference $E_{np} - N_i\epsilon_i$ on N_{xr}, which permits one to determine the values of ϵ_{xr} and ϵ_{xp}. Calculations of the energy/atom for the triangular nanoplatelets with compositions $(MoS_2)_9$, $(MoS_2)_{18}$, $(MoS_2)_{30}$, $(MoS_2)_{45}$, $(MoS_2)_{63}$, $(MoS_2)_{84}$, and $(MoS_2)_{108}$ were carried out that resulted in $\epsilon_{xr} = -2.1323$ H/atom and $\epsilon_{xp} = -2.1303$ H/atom (Figure 12).

Figure 13 illustrates the dependence of the energy per atom of the MoS_2 nanoplatelets and octahedral MoS_2 fullerenes with various numbers of layers (k). The energies follow roughly a $1/N$ behavior. Single-walled MoS_2 nanooctahedra were found to be less stable than nanoplatelets over the entire range of N.

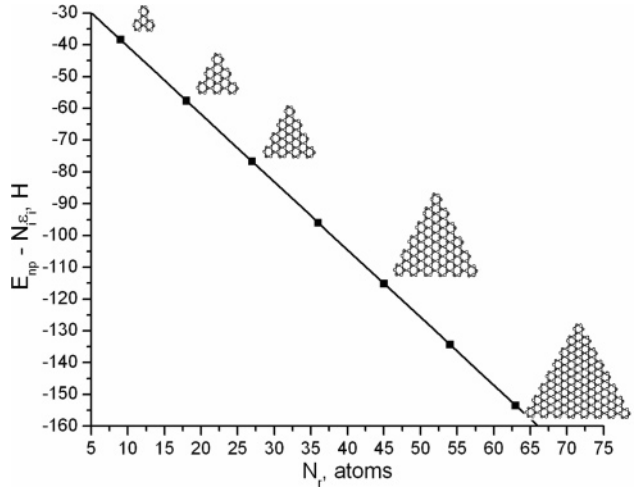

Figure 12. Relation between the energies of the MoS_2 nanoplates E_{np} and the number of atoms with dangling bonds N_r. N_i and ϵ_i are the number of inner atoms and their energies, respectively (eq 5) (DFTB calculations).

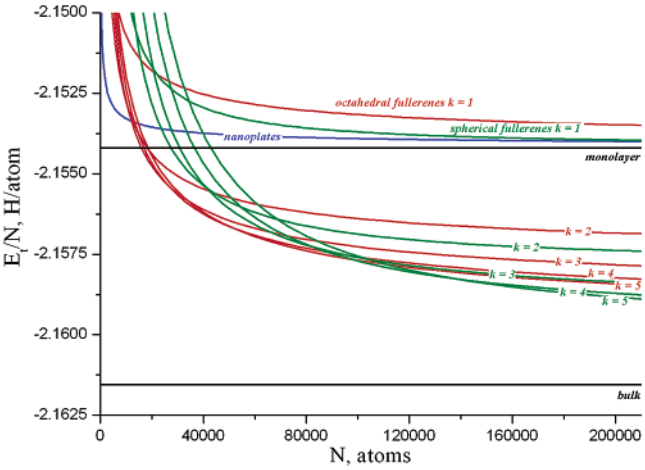

Figure 13. Energies per atom E_t/N of the multilayered fullerenes of octahedral or spherical shape with the number of shells k and for triangular nanoplates of stoichiometric molybdenum disulfide as a function of the number of atoms N in comparison with the energy of a bulk MoS_2 monolayer, as obtained from DFTB calculations and estimations via eqs 4, 6, and 9.

The calculations furthermore indicate that the stability of the nanooctahedra increases proportionally with the number of layers k. These observations are confirmed with the published experimental data[24,27] and the (experimental) results reported below. In contrast to the carbon analogues, such as C_{60} and C_{70}, single-walled nanostructures of the d-metal dichalcogenides have not been observed so far. Furthermore, multilayered octahedral fullerenes of MoS_2 are more stable than nanoplatelets for $N \geq 12\,500$ atoms. (Only single-layered nanoplatelets were considered here, because it is not expected that (multilayered) nanoplatelets are formed due to the weakness of the interlayer interaction.)

Through the use of the present approach it is also possible to estimate the relative stabilities of the quasi-spherical inorganic fullerene-like nanoparticles in comparison with those of the octahedral particles. The exact nature, number, and distribution of the defects causing the spherocity of these MoS_2 particles are not known. However, one may assume that the number of defects is quite small in comparison to the total number of atoms in the nanoparticle. For instance, one can see from eq 3 that, for the octahedral fullerenes, the contribution of the square-like defects providing the curvature of MoS_2 layers to the total energy is decreasing very rapidly with an increasing number of atoms N.

To calculate the energy of the quasi-spherical multiwalled fullerene-like nanoparticles the following model was used. The energy of a single-walled nanotube can be written as[6,7]

$$\frac{E_t}{N} = \epsilon_i + \frac{\alpha}{R^2} \tag{7}$$

An analysis of the relative stability of tubes and hollow spherical nanoparticles using elasticity theory[25] shows that the strain energy of spherical particles is larger compared to that of tubes with the same radii by a factor $2(1+\sigma)$, where σ is the Poisson ratio. DFTB calculations give $\sigma = 0.26$ for single-walled MoS_2 nanotubes. The number of atoms N in a hollow spherical fullerene-like shell is proportional to R^2. Therefore, the energy per atom may be written as

$$\frac{E_f}{N} = \epsilon_i + 2(1+\sigma)\frac{\alpha}{R^2} = \epsilon_i + \frac{\beta}{N} \tag{8}$$

The validity of eqs 7 and 8 was confirmed for carbon nanotubes and carbon fullerenes.[38] Through the use of the data from the previous investigations of MoS_2 nanotubes,[6,7] it was found that $\beta = 50.3919$ H. Taking into account the van der Waals interactions between the shells these estimations can be extended to the case of multilayered hollow spherical nanoparticles

$$\frac{E_f}{N} = \epsilon_i + \frac{\beta k}{\sum_{j=1}^{k} N_j} + \frac{k-1}{k}\epsilon_{vdW} \tag{9}$$

The relation between the number of atoms of two neighboring fullerene-like shells (N_j and N_{j-1}) is determined using the relation

$$\sqrt{N_j} - \sqrt{N_{j-1}} = \sqrt{\sqrt{3}\pi}\,\frac{c}{a}$$

where c and a are the lattice constants of bulk MoS_2. Figure 13 illustrates the size dependence of the energy per atom for hollow and spherical MoS_2 nanoparticles with different numbers of layers k. One can see that for spherical nanoparticles a similar behavior to that for octahedral nanoparticles is obtained; i.e., single-walled nanoparticles are less stable than nanoplatelets over the entire range of N. Furthermore, the stability of the hollow spherical nanoparticles increases considerably with increasing k.

However, the most important conclusion from Figure 13 is the presence of the "crossover points" between the energy curves of the nanooctahedra and the nanospheres at values of N on the order of a few 10^4 atoms. Thus, the present calculations show that—in agreement with the experimental observations—there is a very peculiar dependence of the nanocluster topology on their size. In particular, multiwalled octahedral MoS_2 fullerenes exhibit a window of stability, which is intermediate between a few hundred and a few thousand atoms, where nanoplatelets are the most stable structures, and quasi-spherical fullerene-like particles of MoS_2, which become stable beyond 10^5 atoms. The lower limit of stability of the nanooctahedra stems from the elastic strain, which does not allow the nanoclusters to fold into closed-cage structures of a diameter smaller than 2−3 nm. As for the upper limit of stability of the nanooctahedra, continuum theory predicts that closed-cage nanostructures with

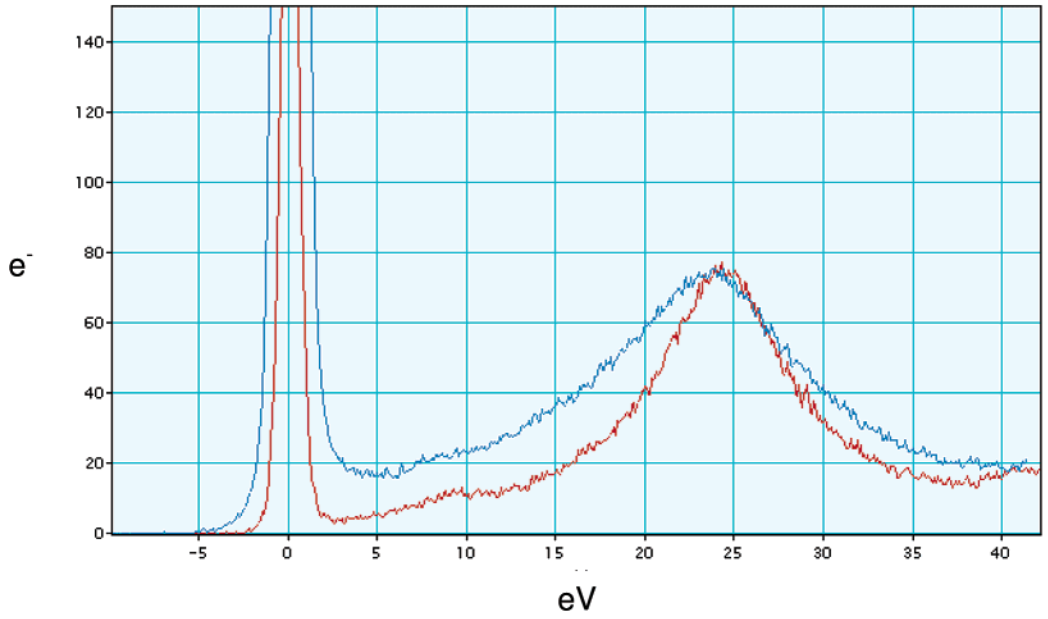

Figure 14. EELS spectra of multilayer IF-MoS_2 nanoparticles (red) and molybdenum sulfide nanooctahedra (blue).

large diameters fold evenly rather than having corners with sharp angles.[25] It is most likely that by adding more layers to the nanoplatelets and to the quasi-spherical fullerene-like MoS_2 nanoparticles the window of stability for the nanooctahedra will become narrower, and perhaps better fitting to the experimental data would thus be obtained.

The experimental part of this work is focused on the synthesis and analysis of laser-ablated MoS_2 nanooctahedra as well as quasi-spherical (multilayer) fullerene-like MoS_2 nanoparticles (>30 nm) and 2H−MoS_2 platelets. The analysis was done using TEM, HRTEM, and associated techniques, such as electron diffraction and EELS. Pairs and even triples of nanooctahedra with either a common wall (facet) or edge were also observed. Many of the nanooctahedra were nonperfect. For example, in some of the nanooctahedra the corners were rounded rather than being sharp. In many cases at least one out of the four projected angles of the nanooctahedron was rounded and not faceted.

HRTEM imaging and Fourier filtering of a large number of molybdenum sulfide nanoparticles with octahedral morphologies revealed that in accordance with bulk MoS_2 the atoms are arranged in a hexagonal pattern. These hexagonal patterns were compared with a HRTEM image simulation of MoS_2 platelets viewed down the [001] direction. It seems that in many images the Mo−S bond is pointing toward the apex of the octahedron (or perpendicular to the edges), suggesting that perhaps case I is more abundant or favorable than case II (Figure 3).

EELS analysis of MoS_2 samples was undertaken. The sample containing 2H−MoS_2 platelets showed a high signal-to-noise ratio and very distinct Mo ($L_{3,2}$) and S (K) peaks. The S/Mo ratio was determined by integration of the S−K edge relative to the Mo−$L_{3,2}$ edge. In the case of the 2H−MoS_2 platelets two configurations were analyzed with the platelet lying down ($\parallel c$) or perpendicular to the beam ($\perp c$), i.e., the molecular MoS_2 sheets parallel to the beam. In this case the EELS signal and consequently the S/Mo ratio revealed a strong orientation dependence. For the $\parallel c$ orientation an average ratio of 1.95 ± 0.2 was obtained while in the $\perp c$ orientation the ratio was 1.65 ± 0.2. In the case of the multilayer fullerene-like nanoparticles (>30 nm in size) a ratio of 1.6 ± 0.1 was obtained. These latter results are orientation-independent and are therefore more useful as a reference for the determination of the S/Mo stoichiometry in the nanooctahedra.

Laser-ablated samples containing the nanooctahedra were also analyzed. The analyzed area in this case was no larger than 50 nm^2 and typically contained two to four nanooctahedra. Given the fact that the nanooctahedra themselves are 4 nm high each, the cross-section of the samples toward the beam was extremely small. The noise level was very high, and therefore the background subtraction became a nontrivial issue.

However, clearly the sulfur peak was much reduced compared to that of the fullerene-like nanoparticles 50 nm in size. Through the use of the results of the nested fullerene-like particles (>30 nm) as a reference for EELS quantification where no orientation effect should occur, then a ratio of 1.3 ± 0.1 was calculated; thus a sulfur deficiency of approximately 35% is obtained in the nanooctahedra. To avoid beam damage, the beam was not allowed to be focused on small areas (<50 nm^2). Several tests were done to confirm that no beam damage took place during the EELS analysis. The measured sulfur deficiency, which is much too large in comparison to the theoretically predicted deviation, may reflect also the loss of sulfur during the laser ablation process, which leads to the formation of some unspecified amorphous material between the nanooctahedra.

Quantitative analysis of the low energy loss spectra was undertaken as shown in Figure 14. The plasmonic part of the spectrum of the nanooctahedra was compared with that of the larger fullerene-like nanoparticles (and the bulk 2H−MoS_2 platelets). The statistically averaged peak of the IF-MoS_2 nanoparticles occurred at 24.6 ± 0.3 eV, and its full width at half-maximum (fwhm) was 9.8 eV; for the nanooctahedra it was 23.7 ± 0.4 and 16.9 eV, respectively. The broadening of the plasmon peak in the octahedra is probably due to a large contribution from the surface plasmon around 16.0 eV.[39] This may also be the reason for the shift of the plasmon peak to lower energies. The overall similarity between the two spectra is indicative of the close relationship between bulk 2H−MoS_2 platelets and the molybdenum sulfide nanooctahedra.

A quantitative analysis of the nanooctahedra's edge lengths was performed in a procedure similar to that described by Parilla et al.[27] The edge length of the octahedron, which is imaged by its projection, is actually $\sqrt{2}$ times the length of the vector connecting the vertex with the geometric center of the octahedron. One can measure the length of the diagonal between two opposite vertexes, multiplied by $\sqrt{2}$, and the result would

TABLE 1: Average Edge Length and the Total Number of Atoms ($N_{Mo+S/Se}$) for the $MoS_2/MoSe_2$ Nanooctahedra[a]

layer no.	MoS_2 average and STD (in units of *a*)	MoS_2 total no. of atoms in shell: average-sized nanooctahedron ± STD	$MoSe_2$ average and STD (in units of *a*)	$MoSe_2$ total no. of atoms in shell: average-sized nanooctahedron ± STD
4	15.8 ± 4.6	3048 (1428, 4776)	13.5 ± 6.0	2328 (744, 4776)
3	13.3 ± 3.5	2004 (1176, 3444)	11.6 ± 5.1	1704 (564, 3444)
2	9.9 ± 3.1	1176 (564, 2004)	8.4 ± 4.5	744 (168, 2004)
1	6.2 ± 3.1	408 (84, 948)	3.4 ± 1.1	84 (33, 276)
average	10.8 ±4.4	1428 (408, 2676)	9.9 ± 5.8	1176 (168, 3048)

[a] The minimum and maximum number of atoms in a shell are in parentheses. Standard deviation is abbreviated as STD.

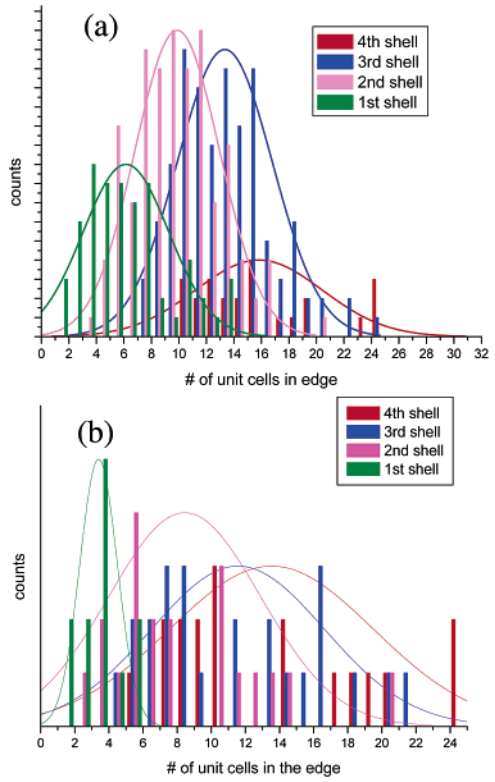

Figure 15. Histogram of nanooctahedra edge lengths (in unit cells) by shell for (a) 72 MoS_2 particles and (b) 16 $MoSe_2$ particles.

contribute half a count to the size histogram. The results were all divided by the bulk lattice constant *a* (3.16 Å), enabling comparison of nanooctahedra of MoS_2 (72 units) and its analogous material $MoSe_2$ (a = 3.29 Å, 16 units). Each octahedron consisted of a few layers. Figure 15 presents a histogram of edge length by shell (the first one being the most inner one) for MoS_2 and for $MoSe_2$ nanooctahedra. The results of this analysis are summarized in Table 1. The experimental errors of the length measurement can be estimated as $\pm^1/_2$ unit cell. In the last row of Table 1 the average shell size was obtained by summing over all the nanooctahedra of this study. The largest nanooctahedra observed were 24−25 unit cells long in their outer shell, corresponding to 2300−2496 Mo atoms (or in total 25 000 atoms for a five-layered nanooctahedron). This makes about one-quarter of the maximum value calculated by the above model (Figure 13). Given the level of approximations in the model, the agreement between experiment and theory is more than satisfactory.

The difference in the edge lengths of adjacent shells is usually much smaller than that calculated using geometrical considerations, which takes into account an ideal octahedron. The observed 3−4 unit cells difference can be compared to the value of 4.76 derived from geometrical considerations, which is in agreement with the results of Parilla et al.[27] Smaller-sized structures exist in the center of the octahedra and may have edge lengths of 2−3 unit cells.

Note that, in accordance with the model calculations presented above, the bulk synthesis of IF-MoS_2[26] yielded closed multilayered and hollow (fullerene-like) nanoparticles 30 nm and above with quasi-spherical shapes. No nanooctahedra were observed in the synthesis of IF-MoS_2 from the respective molybdenum oxide,[26] suggesting that in agreement with the calculations the nanooctahedra possess a higher energy as compared with the nested fullerene-like MoS_2 nanoparticles >30 nm in size. Also, the synthetic route involves nucleation of MoS_2 layers on the MoO_x nanoparticles' surfaces therefore preventing some energetic configurations, such as the nanooctahedra, from being sampled. More recently, new synthetic strategies for fullerene-like MoS_2 were developed where volatile precursors, such as $Mo(CO)_6$ [40] and $MoCl_5$, [41] reacted with heated sulfur vapor or H_2S at 450−850 °C. These synthetic approaches yielded multilayered (nested) quasi-spherical MoS_2 nanoparticles of a typical size between 20 and 100 nm. No nanooctahedra were observed in these studies either. This body of work indicates that indeed synthetic approaches for IF-MoS_2 involving reaction conditions close to thermodynamic control do not produce the more energetic nanooctahedra. Some faceting of the IF-MoS_2 nanoparticles with 90° inclinations was nevertheless observed in all these reactions.[2]

The observation of nanooctahedra was not limited to MoS_2 and was also common to metal halides, such as $NiCl_2$ and $NiBr_2$,[42] though in smaller yields. In the case of $MoSe_2$ the production yield of the nanooctahedra was similar to that of MoS_2. The number of molecular layers in $MoSe_2$ nanooctahedra was usually higher than that observed for MoS_2. In fact, $MoSe_2$ showed an octahedron with five layers, while most of the MoS_2 nanooctahedra contained less than four layers. This corresponds to the stronger interlayer coupling in $MoSe_2$ as compared to that in MoS_2.[43]

The TEM images of $MoSe_2$ also showed triangular structures, suggesting a trigonal biprism or nanotetrahedron three-dimensional (3D) structure (Figure 16). In contrast to MoS_2 where plenty of faceted nanoparticles including the nanooctahedra were found, the laser ablation of WS_2 produced much less faceted closed nanostructures[44] (Figure 16b). Pure spherical morphology was not found in the soot of laser-ablated MoS_2 or $MoSe_2$.

In analogy to previous works,[24,27,28,44] the 3D model of the nanooctahedra was confirmed via tilting experiments at the TEM (Figure 17). Figure 17a shows a TEM micrograph of a three-layer octahedron tilted at various angles, while Figure 17b shows views of the corresponding model structure. The coincidence between the projected structures is quite remarkable, suggesting that the experimentally observed octahedral structures are consistent with the models offered.

4. Conclusions

Atomic models of molybdenum sulfide fullerenes with both stoichiometric and nonstoichiometric compositions were constructed. Their stabilities and electronic properties have been investigated for the first time using the DFTB method depending

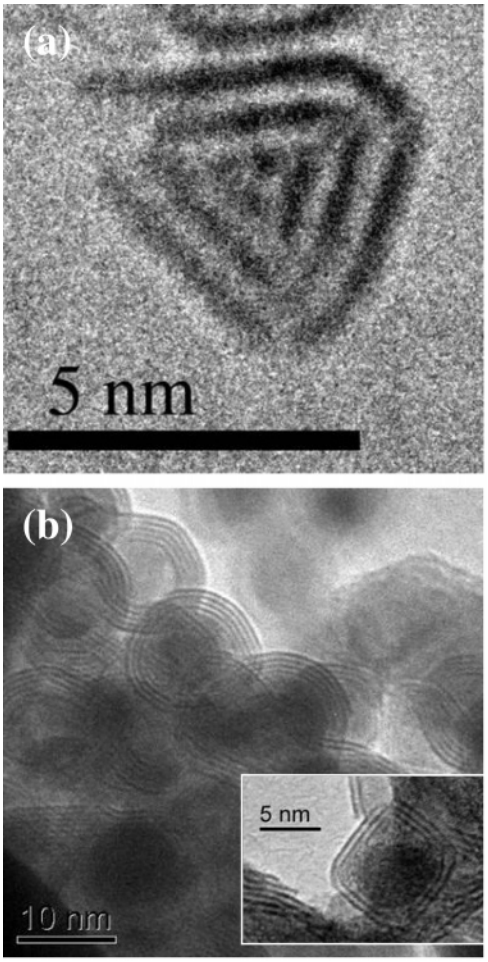

Figure 16. TEM images of particles produced by laser ablation: (a) a triangular projection of a nanotetrahedron of $MoSe_2$, (b) WS_2 spherical nanoparticles, and (inset in b) WS_2 faceted nanoparticles.

on the sizes and stoichiometries of the particles. The present calculations and the MD simulations show that the stoichiometric single-walled MoS_2 fullerenes with octahedral shapes are unstable at least at the considered sizes of a few hundreds of atoms. This instability is attributed to the high strain energies at the corners of the MoS_2 nanooctahedra.

In the range of the cage sizes that were amenable for DFTB calculations (a few hundred atoms), the most stable hollow particles with octahedral shapes can have only nonstoichiometric compositions. Among 14 types of the nonstoichiometric Mo_nS_m nanooctahedra were found the most stable configurations. Moreover, the analysis shows that the construction of corners or edges plays a much more important role in the stability of fullerenes than even the presence of atoms with an unusual atomic coordination in a fullerene-like cage.

Furthermore, a phenomenological model for the energetics of multilayered and stoichiometric molybdenum sulfide nanooctahedra was developed, and the results were compared with those of nanoplatelets of the same composition. This analysis shows that multiwalled MoS_2 nanooctahedra might be expected to become stable for cages with more than $\sim$12 000 atoms. When the sizes of the multiwalled hollow cages increase beyond a few tens of thousands of atoms the octahedral shape loses in competition with nested (multiwalled) spherical shape nanoparticles.

The electronic properties of the small hollow nanocages of molybdenum sulfide are found to be rather different from bulk or even nanotubular MoS_2. All hollow octahedral Mo_nS_m nanoparticles exhibit a small difference between the highest occupied and the lowest unoccupied energy levels composed mainly of 4d Mo states. All the MoS_2 nanooctahedra exhibit the similar DOS spectra, independent of their stoichiometry and size. However, the detailed profile of the DOS near the HOMO depends considerably on the specific structure and the size of the particles.

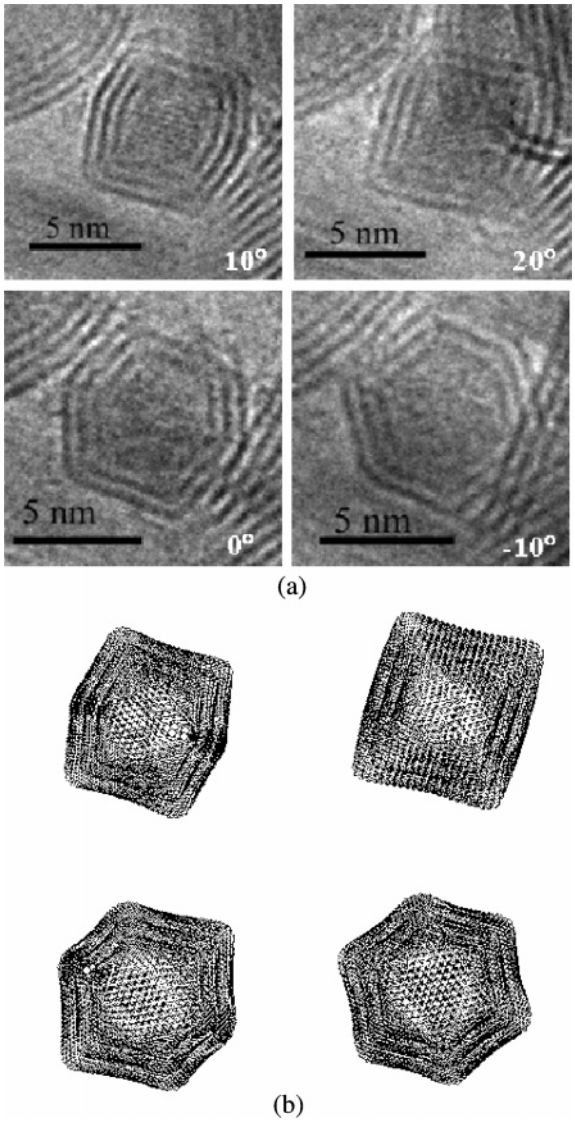

Figure 17. Tilting experiments of MoS_2 nanooctahedra in TEM and corresponding images of the atomic model for a $(MoS_2)_{784}@(MoS_2)_{1296}@(MoS_2)_{1936}$ fullerene. (a) TEM imaging of a three-layered nanooctahedron in various tilting angles. (b) Corresponding images of the atomic model for a $(MoS_2)_{784}@(MoS_2)_{1296}@(MoS_2)_{1936}$ octahedral fullerene. Note the visual similarity between (a) the experimentally observed and (b) the model structures.

On the experimental side, targets of MoS_2 and $MoSe_2$ were laser-ablated and analyzed mostly through TEM. Numerous nanooctahedra were found in the ablated samples, and they were carefully analyzed statistically. This analysis shows that, in qualitative agreement with the theoretical analysis, multilayer nanooctahedra of MoS_2 with 1000−25 000 atoms (Mo + S) are stable. Furthermore, this and previous work show that beyond $\sim 10^5$ atoms fullerene-like structures with quasi-spherical shapes and 30−100 layers are stable. Laser-ablated WS_2 samples yielded much less faceted and sometimes spherically symmetric nanocages.

It is hoped that the present results will serve in the next detailed experimental investigations, which will lead to elucida-

tion of the structure and the physical properties of the inorganic fullerenes and related nanostructures based also on other compounds.

Acknowledgment. This work was supported by the following agencies: German−Israeli Foundation (GIF), Minerva Foundation (Munich), GMJ Schmidt Minerva Center for Supramolecular Architectures, and the Israel Science Foundation.

References and Notes

(1) Tenne, R.; Margulis, L.; Genut, M.; Hodes, G. *Nature* **1992**, *360*, 444.
(2) Margulis, L.; Salitra, G.; Talianker, M.; Tenne, R. *Nature* **1993**, *365*, 113.
(3) Feldman, Y.; Wasserman, E.; Srolovitz, D. J.; Tenne, R. *Science* **1995**, *267*, 222.
(4) Tenne, R. *Chem.−Eur. J.* **2002**, *8*, 5296.
(5) Rao, C. N. R.; Nath, M. *Dalton Trans.* **2003**, 1.
(6) Seifert, G.; Terrones, H.; Terrones, M.; Jungnickel, G.; Frauenheim, T. *Phys. Rev. Lett.* **2000**, *85*, 146.
(7) Seifert, G.; Köhler, T.; Tenne, R. *J. Phys. Chem. B* **2002**, *106*, 2497.
(8) (a) Kaplan-Ashiri, I.; Cohen, S. R.; Gartsman, K.; Rosentsveig, R.; Seifert, G.; Tenne, R. *J. Mater. Res.* **2004**, *19*, 454. (b) Kaplan-Ashiri, I.; Cohen, S. R.; Gartsman, K.; Ivanovskaya, V.; Heine, T.; Seifert, G.; Kanevsky, I.; Wagner, H. D.; Tenne, R. *Proc. Natl. Acad. Sci. U.S.A.* **2006**, *103*, 523.
(9) Rapoport, L.; Fleischer, N.; Tenne, R. *J. Mater. Chem.* **2005**, *15*, 1782.
(10) Zak, A.; Feldman, Y.; Alperovich, V.; Rosentsveig, R.; Tenne, R. *J. Am. Chem. Soc.* **2000**, *122*, 11108.
(11) Li, X. L.; Li, Y. D. *Chem.−Eur. J.* **2003**, *9*, 2726.
(12) Mastai, Y.; Homyonfer, M.; Gedanken, A.; Hodes G. *Adv. Mater.* **1999**, *11*, 1010.
(13) Xiong, Y.; Xie, Y.; Li, Z.; Li, X.; Zhang, R. *Chem. Phys. Lett.* **2003**, *382*, 180.
(14) Sano, N.; Wang, H.; Chhowalla, M.; Alexandrou, I.; Amaratunga, G. A. J.; Naito, M.; Kanki, T. *Chem. Phys. Lett.* **2003**, *368*, 331.
(15) Feldman, Y.; Frey, G. L.; Homyonfer, M.; Lyakhovitskaya, V.; Margulis, L.; Cohen, H.; Hodes, G.; Hutchison, J. L. Tenne, R. *J. Am. Chem. Soc.* **1996**, *118*, 5362.
(16) (a) Hersfinkel, M.; Gheber, L. A.; Volterra, V.; Hutchison, J. L.; Margulis, L.; Tenne, R. *J. Am. Chem. Soc.* **1994**, 116, 1914. (b) Scheffer, L.; Rosentsveig, R.; Margolin, A.; Popovitz-Biro, R.; Seifert, G.; Cohen, S. R.; Tenne, R. *Phys. Chem. Chem. Phys.* **2002**, *4*, 2095. (c) Azulay, D.; Kopnov, F.; Tenne, R.; Balberg, I.; Millo, O. *Nano Lett.* **2006**, *6*, 760.
(17) (a) Remskar, M.; Mrzel, A.; Sanjines, R.; Cohen, H.; Levy, F. *Adv. Mater.* **2003**, *15*, 237. (b) Hassanien, A.; Tokumoto, M.; Mrzel, A.; Mihailovic, D.; Kataura, H. *Physica E* **2005**, *29* 684−688.
(18) Frey, G. L.; Elani, S.; Homyonfer, M.; Feldman, Y.; Tenne, R. *Phys. Rev. B* **1998**, *57*, 6666.
(19) (a) Frey, G. L.; Tenne, R.; Matthews, M. J.; Dresselhaus, M. S.; Dresselhaus, G. *Phys. Rev. B* **1999**, *60*, 2883. (b) Rafailov, P. M.; Thomsen, C.; Gartsman, K.; Kaplan-Ashiri, I.; Tenne, R. *Phys. Rev. B* **2005**, *72*, 205436. (c) Luttrell, R. D.; Brown, S.; Cao, J.; Musfeldt, J. L.; Rosentsveig, R.; Tenne, R. *Phys. Rev. B* **2006**, *73*, 035410.
(20) Zak, A.; Feldman, Y.; Lyakhovitskaya, V.; Leitus, G.; Popovitz-Biro, R.; Wachtel, E.; Cohen, H.; Reich, S.; Tenne, R. *J. Am. Chem. Soc.* **2002**, *124*, 4747.
(21) (a) Rapoport, L.; Fleischer, N.; Tenne, R. *J. Mater. Chem.* **2005**, *15*, 1782. (b) Cizaire, L.; Vacher, B.; Le Mogne, T.; Martin, J. M.; Rapoport, L.; Margolin, A.; Tenne, R. *Surf. Coat. Technol.* **2002**, *160*, 282.
(22) Zhu, Y. Q.; Sekine, T.; Li, Y. H.; Fay, M. W.; Zhao, Y. M.; Patrick Poa, C. H.; Wang, W. X.; Roe, M. J.; Brown, P. D.; Fleischer, N.; Tenne, R. *J. Am. Chem. Soc.* **2005**, *127*, 16263.
(23) Tenne, R. *Adv. Mater.* **1995**, *7*, 965.
(24) Parilla, P. A.; Dillon, A. C.; Jones, K. M.; Riker, G.; Schulz, D. L.; Ginley, D. S.; Heben, M. J. *Nature* **1999**, *397*, 114.
(25) Srolovitz, D. J.; Safran, S. A.; Homyonfer, M.; Tenne, R. *Phys. Rev. Lett.* **1995**, *74*, 1779.
(26) Therese, H. A.; Zink, N.; Kolb, U.; Tremel, W. *Solid State Sci.* **2006**, *8*, 1133.
(27) Parilla, P. A.; Dillon, A. C.; Parkinson, B. A.; Jones, K. M.; Alleman, J.; Riker, G.; Ginley, D. S.; Heben, M. J. *J. Phys. Chem. B* **2004**, *108*, 6197.
(28) Ascencio, J. A.; Perez-Alvarez, M.; Molina, L. M.; Santiago, P.; Jose-Yacaman, M. *Surf. Sci.* **2003**, *526*, 243.
(29) Enyashin, A. N.; Ivanovskaya, V. V.; Makurin, Yu. N.; Ivanovskii, A. L. *Inorg. Mater.* **2004**, *40*, 466.
(30) Porezag, D.; Frauenheim, T.; Köhler, T.; Seifert, G.; Kashner, R. *Phys. Rev. B* **1995**, *51*, 12947.
(31) Seifert, G.; Porezag, D.; Frauenheim, T. *Int. J. Quantum Chem.* **1996**, *58*, 185.
(32) Seifert, G.; Vietze, K.; Schmidt, R. *J. Phys. B: At., Mol. Opt. Phys.* **1996**, *29*, 5183.
(33) Singh, D. M. D. J.; Pradeep, T.; Bhattacharjee, J.; Waghmare, U. V. *J. Phys. Chem. A* **2005**, *109*, 7339.
(34) Enyashin, A. N.; Seifert,G. *Phys. Status Solidi B* **2005**, *242*, 1361.
(35) Helveg, S.; Lauritsen, J. V.; Lægsgaard, E.; Stensgaard, I.; Nørskov, J. K.; Clausen, B. S.; Topsøe, H.; Besenbacher, F. *Phys. Rev. Lett.* **2000**, *84*, 951.
(36) Bollinger, M. V.; Lauritsen, J. V.; Jacobsen, K. W.; Nørskov, J. K.; Helveg, S.; Besenbacher, F. *Phys. Rev. Lett.* **2001**, *87*, 196803.
(37) Fuhr, J. D.; Sofo, J. O.; Saul, A. *Phys. Rev. B* **1999**, *60*, 8343.
(38) Robertson, D. H.; Brenner, D. W.; Mintmire, J. W. *Phys. Rev. B* **1992**, *45*, 12592.
(39) Cohen, H.; Maniv, T.; Tenne, R.; Rosenfeld Hacohen, Y.; Stephan, O.; Colliex, C. *Phys. Rev. Lett.* **1998**, *80*, 782.
(40) Etzkorn, J.; Therese, H. A.; Rocker, F.; Zink, N.; Kolb, U.; Tremel, W. *Adv. Mater.* **2005**, *17*, 2372.
(41) Deepak, F. L.; Margolin, A.; Bar-Sadan, M.; Popovitz-Biro, R.; Tenne, R. *NANO* **2006**, *1*, 167.
(42) Bar-Sadan, M.; Popovitz-Biro, R.; Prior, Yehiam; Tenne, R. *Mater. Res. Bull.* **2006**, *41*, 2137.
(43) *Electrons and Phonons in Layered Crystal Structures*; Wieting, T. J., Schluter, M., Eds.; D. Reidel Publishing Company: Dordrecht, The Netherlands, 1976; Vol. 3, p 359.
(44) Sen, R.; Govindaraj, A.; Suenaga, K.; Suzuki, S.; Kataura, H.; Iijima, S.; Achiba, Y. *Chem. Phys. Lett.* **2001**, *340*, 242.